

Supporting Information

Terminal substituent induced differential aggregation and sensing properties: A case study of neutral benzimidazole based urea receptors

Rubi Moral, Oiyao Appun Pegu, and Gopal Das*

Department of Chemistry, Indian Institute of Technology Guwahati,

Assam-781039, India

E-mail: gdas@iitg.ac.in

EXPERIMENTAL SECTION

All reagents and solvents were obtained from commercial sources and used as received without further purification. 2-(1H-benzimidazol-2-yl)aniline, naphthyl isocyanate and 3-cyanophenyl isocyanate and different Tetrabutylammonium salts (TBA salts) were purchased from TCI and Sigma-Aldrich and used as received. Solvents for synthesis and crystallization experiments were purchased from Merck, India, and used as received. NMR spectra were recorded on Bruker Advance 500/600 MHz instruments in DMSO-d₆, and chemical shifts were recorded in parts per million (ppm) on the scale using tetramethylsilane [Si(CH₃)₄] or a residual solvent peak as a reference. The following abbreviations are used to describe spin multiplicities in ¹H NMR spectra: s = singlet; d = doublet; t = triplet; q = quartet, m = multiplet. High-resolution mass spectrometry of **R1** and **R2** were carried out on an Agilent QToF mass spectrometer. IR spectra of all of the two receptors (**R1** and **R2**) and their complexes with SO₄²⁻/HSO₄⁻ were recorded on PerkinElmer FT-IR spectrometer as KBr disks in the range 4000–450 cm⁻¹. The UV-Visible absorption spectra were archived on a Perkin-Elmer Lambda-750 UV-Vis spectrophotometer using 10 mm path length quartz cuvettes in 250-700 nm wavelengths. Baseline correction was applied for all spectra. Fluorescence emission spectra were documented on a Horiba Fluoromax-4 spectrofluorometer using 1 cm path length quartz cuvettes having a slit width of 5 nm at 298 K. The morphology of the aggregated species was investigated by using FESEM imaging studies by the drop (1 mM) cast method on glass plates covered with Al-foil using Gemini 300 FESEM (Carl Zeiss) and Sigma 300 FESEM (10000KX).

Synthetic details

R1: 2-(1H-benzimidazol-2-yl)aniline (500 mg, 2.39 mmol, 1 equiv.) was placed in a 50 mL round-bottomed flask and dissolved in dichloromethane (DCM) (15 mL). A solution of naphthyl isocyanate (340 mg, 2.39 mmol, 1 equiv.) was added into the flask in dropwise manner. The reaction was stirred at room temperature for 12 hours. The precipitates were separated by filtration and washed with DCM (30 mL) and diethyl ether (30 mL). The obtained white powder was further dried over vacuum dried and isolated as compound **R1**. Yield, 90%. ¹H NMR (500 MHz, DMSO-d₆) δ 12.97 (s, 1H), 12.01 (s, 1H), 9.42 (s, 1H), 8.48 (d, J = 8.4 Hz, 1H), 8.15 (d, J = 8.2 Hz, 1H), 7.99 (t, J = 8.2 Hz, 2H), 7.85 (d, J = 8.2 Hz, 1H), 7.65 (d, J = 7.3 Hz, 1H), 7.58-7.50 (m, 4H), 7.42 (dt, J = 15.3, 7.9 Hz, 2H), 7.24 (t, J = 7.4 Hz, 1H), 7.20-7.12 (m, 2H). ¹³C NMR (500 MHz, DMSO) δ 154.68, 151.29, 142.66,

139.98, 134.60, 134.44, 133.99, 130.71, 129.68, 128.58, 127.78, 126.52, 126.37, 126.34, 125.93, 123.55, 123.52, 123.50, 122.21, 121.71, 120.72, 119.21, 115.72, 111.67. **FT-IR** spectra (KBr pellet used): 3226 cm^{-1} vs (urea N–H), 3000 cm^{-1} vs (aromatic C–H), 1653 cm^{-1} vs (urea C=O). **ESI-MS** (positive mode, m/z): calculated for $\text{C}_{24}\text{H}_{18}\text{N}_4\text{O}$: 378.1481. Found: 379.3227 [M + H⁺]. m.p: 193°C.

R2: 2-(1H-benzimidazol-2-yl)aniline (500 mg, 2.39 mmol, 1 equiv.) was placed in a 50 mL round-bottomed flask and dissolved in dichloromethane (DCM) (15 mL). A solution of 3-cyanophenyl isocyanate (344.4 mg, 2.39 mmol, 1 equiv.) was added into the flask in dropwise manner. The reaction was stirred at room temperature for 12 hours. The precipitates were separated by filtration and washed with DCM (30 mL) and diethyl ether (30 mL). The obtained white powder was further dried over vacuum dried and isolated as compound **R2**. Yield: 80%. **¹H NMR** (600 MHz, DMSO-d₆) δ 13.10 (s, 1H), 12.22 (s, 1H), 10.08 (s, 1H), 8.39 (s, 1H), 8.10 - 8.04 (m, 2H), 7.82 (d, J = 8.0 Hz, 2H), 7.60 (s, 1H), 7.55 - 7.50 (m, 1H), 7.49-7.44 (m, 2H), 7.30 (s, 2H), 7.23-7.18 (m, 1H). **¹³C NMR** (600 MHz, DMSO) δ 153.08, 151.37, 141.36, 140.73, 139.36, 130.81, 130.70, 130.59, 127.79, 126.20, 125.95, 124.03, 123.69, 122.21, 122.03, 121.60, 120.92, 119.39, 115.88, 112.11, 111.96. **FT-IR** spectra (KBr pellet used): 3338 cm^{-1} vs (urea N–H), 3291 cm^{-1} vs (aromatic C–H), 2256 cm^{-1} (–C≡N) 1688 cm^{-1} vs (urea C=O). **ESI-MS** (positive mode, m/z): calculated for $\text{C}_{21}\text{H}_{15}\text{N}_5\text{O}$: 353.1277. Found: 354.2478 [M + H⁺], m.p: 172°C.

General Procedure for UV-VIS and fluorescence Spectroscopic Studies

Stock solutions of **R1** and **R2** ($5 \times 10^{-3} \text{mol L}^{-1}$) were prepared in DMSO. For aggregation study as well as UV and fluorescence selectivity experiments, the solution of receptors were then diluted to $10 \times 10^{-6} \text{mol L}^{-1}$ with Millipore water by taking only 4 μL of stock solution and making the final volume 2 mL. Stock solutions of different tetrabutylammonium anions ($50 \times 10^{-3} \text{mol L}^{-1}$) were prepared in DMSO. In fluorescence titration experiments, a quartz optical cell of 10 mm pathlength was filled with a 2.0 mL solution of receptors to which various $\text{SO}_4^{2-}/\text{HSO}_4^-$ solutions were gradually added using a micropipette.

Quantum yield calculation

Here, we have utilized the **Parker-Rees method**¹ to calculate the quantum yield of the prepared luminescent materials, using a **0.5 M H₂SO₄ solution of quinine sulphate** as a standard reference. The formula for this calculation is provided as follows:

$$\Phi_s = (A_r F_s n_s^2 / A_s F_r n_r^2) \Phi_r$$

In this equation, Φ_r represents the quantum yield of the quinine sulfate reference solution, while Φ_s represents the quantum yield of the samples (**R1** and **R2**). The absorbance maxima were kept under 0.1 to minimize the reabsorption of fluorescent light that passed through the materials. The values of A_r and A_s correspond to the absorbance of the reference and samples, respectively, whereas F_r and F_s refer to the integrated area of fluorescence intensity for the reference and sample, respectively. The refractive indices of the reference and samples are represented by n_r and n_s , respectively.²

Detection Limit

The detection limit was calculated on the basis of the fluorescence titration. The fluorescence emission spectrum of **R1** and **R2** was measured 10 times, and the standard deviation of blank measurement was estimated. To measure the slope, the fluorescence emission at respective wavelength was plotted as a function of the concentration of $\text{SO}_4^{2-}/\text{HSO}_4^-$ from the titration experiment. The detection limit was then calculated using the following equation:

$$\text{Detection limit} = 3\sigma/k$$

Where σ is the standard deviation of blank measurement, and k is the slope between the fluorescence emission intensity versus $[\text{SO}_4^{2-}/\text{HSO}_4^-]$.

Benesi-Hildebrand plot

Benesi-Hildebrand plot (concentration Vs $(I_{\text{max}} - I_{\text{min}})/(I - I_{\text{min}})$) was employed for the determination of binding constant of our receptors **R1** and **R2** with $\text{SO}_4^{2-}/\text{HSO}_4^-$.

Time response study and rate constant determination

Response time is a crucial factor for the practical application of a sensor. To do so, the receptor **R1** (10 μM) was exposed towards $\text{SO}_4^{2-}/\text{HSO}_4^-$ (10 μM) for 20 min and the emission intensity at 494 nm was recorded. Considering, pseudo-first-order kinetics, the reaction rate constants of **R1** with $\text{SO}_4^{2-}/\text{HSO}_4^-$ anion were determined from the time-dependent fluorescence spectra. The rate constants were experimentally evaluated from the following equation: $\ln (F_t - F_{\text{min}})/F_{\text{min}} = -k't$ where F_t and F_{min} were the corresponding fluorescence intensities at time t and the end of the reactions, respectively, and k' is the rate constant.

¹H NMR titration experiments of R1 and R2

The ¹H NMR (600 MHz) titrations of the receptors were performed with the tetrabutylammonium sulphate/bisulfate salts, in DMSO-*d*₆ at 298K. The preliminary concentrations of the hosts and the guests were, [receptor]₀ = 50mM, and [SO₄²⁻/HSO₄⁺]₀ = 500mM respectively. All the titrations were performed by 10-16 measurements at room temperature, and the peak of DMSO-*d*₆ (at 2.5ppm) was used for an internal reference.

Crystallographic Refinement Details

All the details of the refinement parameters of crystallographic data collection for the free receptors **R1** and **R2** and the anionic complex of **R1** are furnished in **Table S2** and also all of the above given data have been deposited into CCDC. A crystal of proper size was chosen for **R1**, **R2** and the bisulfate complex of **R1**, and all the crystals were dipped into silicon oil prior to mounting into a glass fibre tube. Supernova (a single source at an offset) Eos diffractometer with Mo K α radiation ($\lambda = 0.71073 \text{ \AA}$) source, connected with a CCD region detector was used to collect the X-ray intensity data and with the help of APEX 4 all the data refinement and cell reduction were done. Using a narrow-frame algorithm and XPREP, the frames were combined with the Bruker SAINT software kit, and data were corrected for absorption effects using the Multi-Scan process (SADABS). Using direct methods in XT, version 2014/15, all of the structures were solved and after that, refinement was done using the full-matrix least-squares technique in the SHELXL-2016 and 2018 software packages on F². The positions of the hydrogen atoms were fixed. We used MERCURY 4.2.0 for Windows for the sake of creating structural drawings. The hydrogen atoms were found on a separate Fourier map and refined where it was most advantageous. For all non-hydrogen atoms Anisotropic refinement was employed.

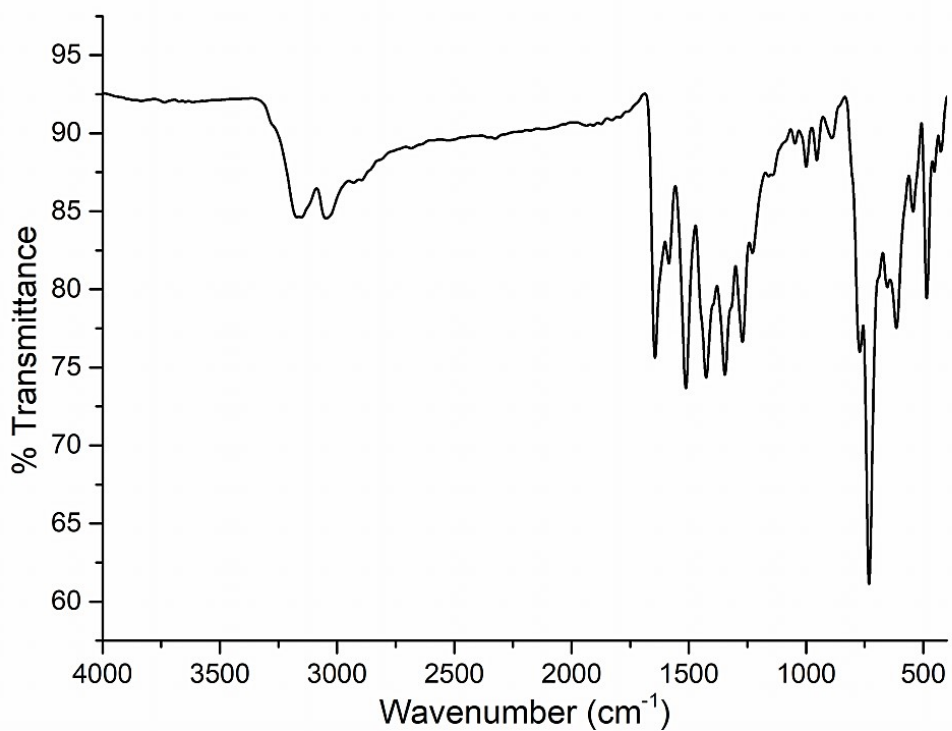


Figure S3: FT-IR spectra of **R1**.

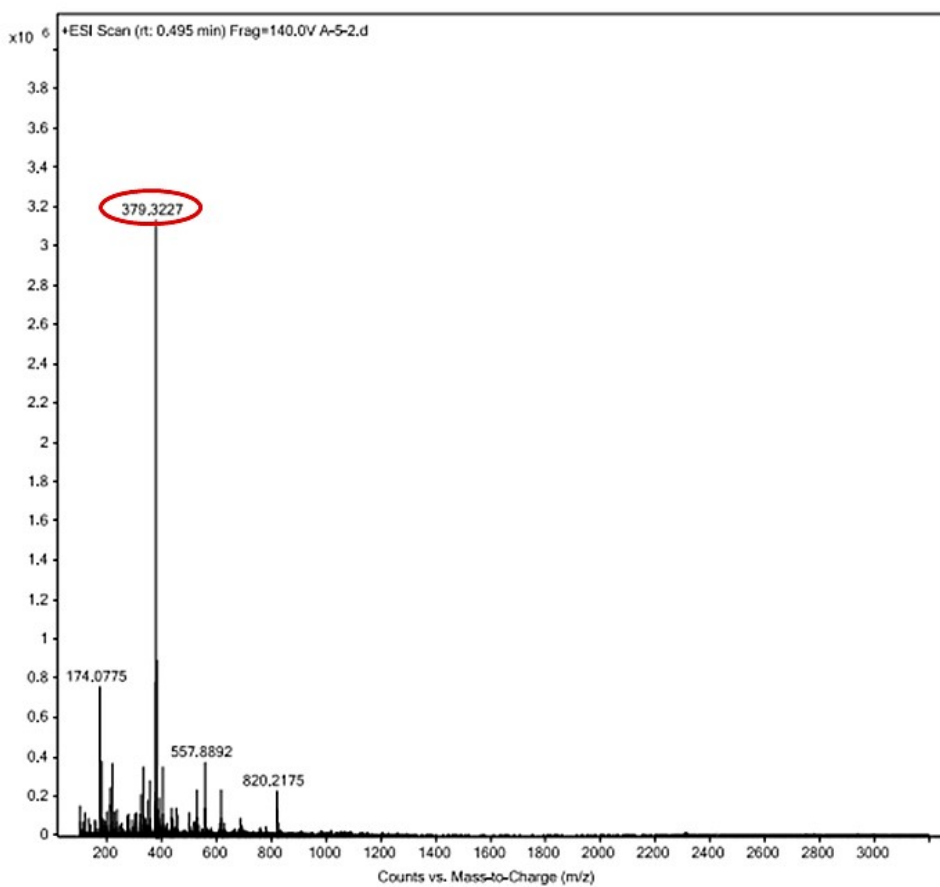


Figure S4. HRMS spectra of **R1** in acetonitrile in positive ionization mode.

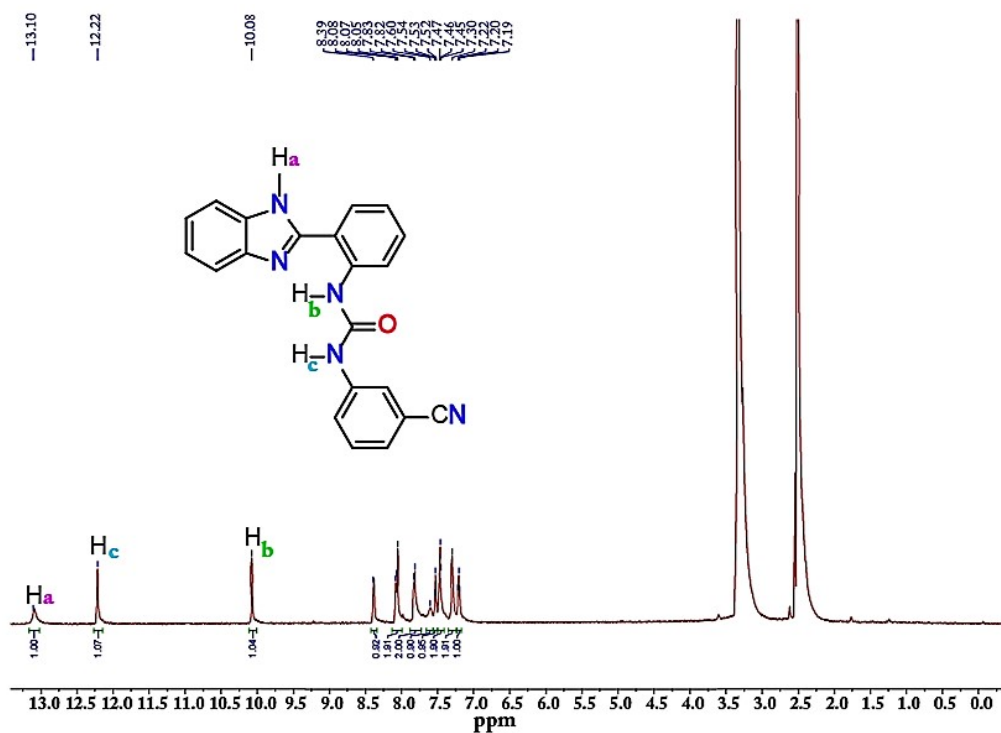


Figure S5: ¹H NMR of **R2** in DMSO-d₆ at room temperature.

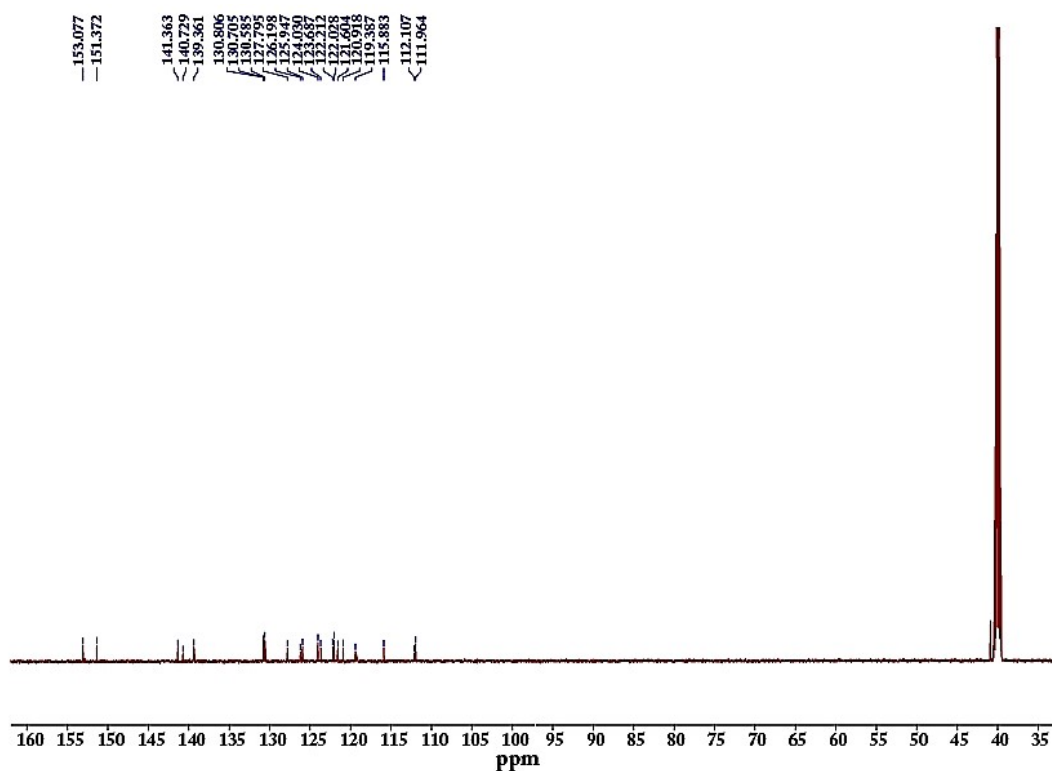


Figure S6: ¹³C NMR of **R1** in DMSO-d₆ at room temperature.

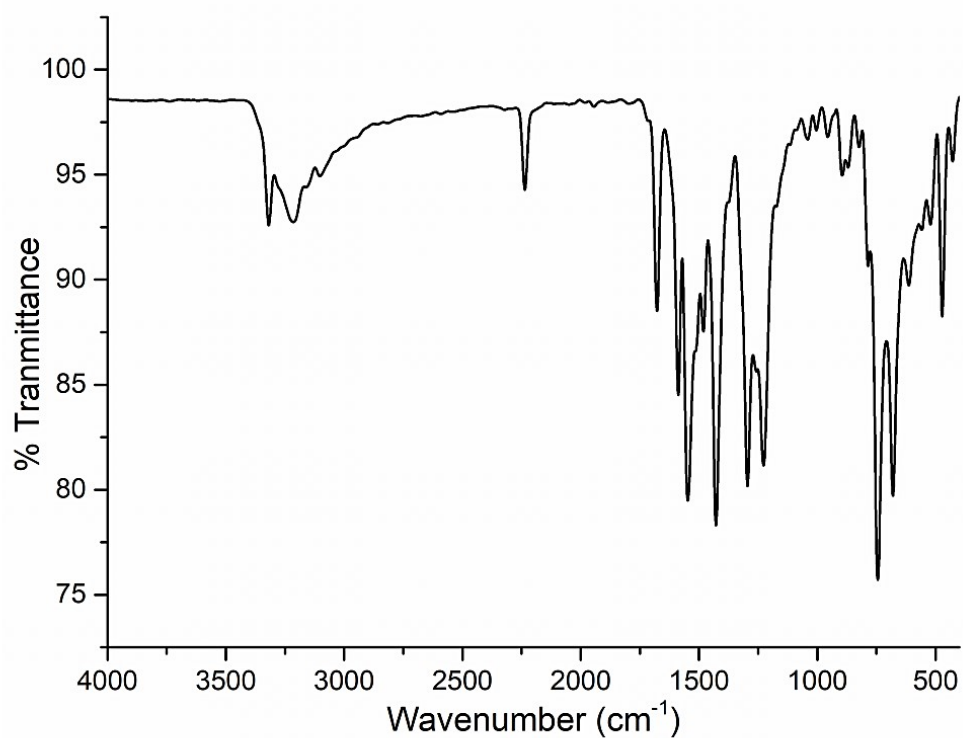


Figure S7: FT-IR spectra of **R2**.

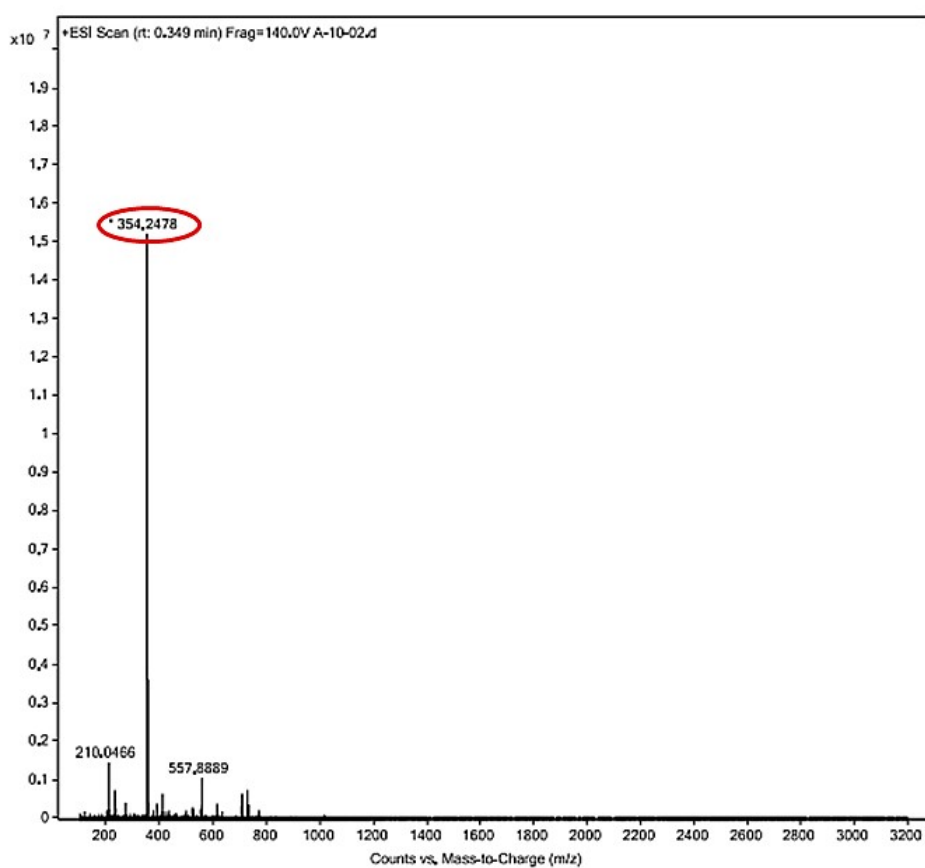


Figure S8. HRMS spectra of **R2** in acetonitrile in positive ionization mode.

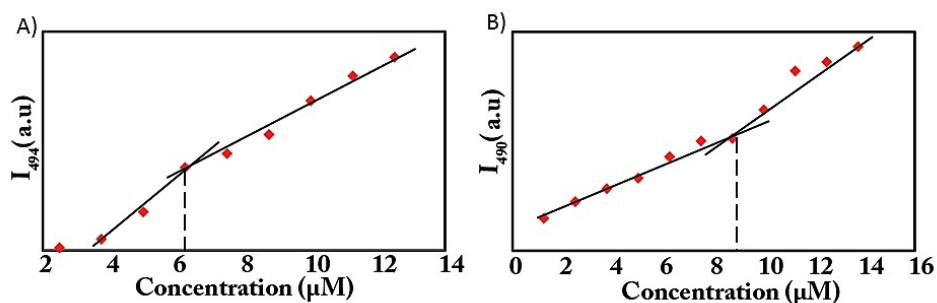


Figure S9. Critical aggregation constant of A) R1 and B) R2.

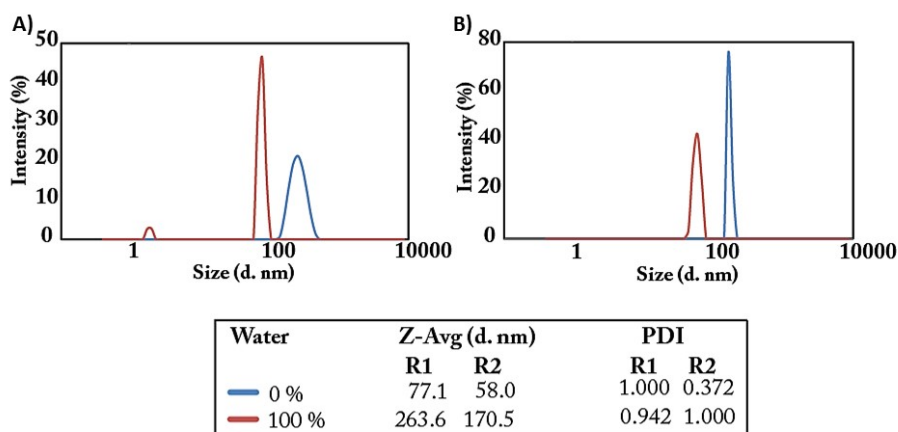


Figure S10. DLS output of A) R1 and B) R2.

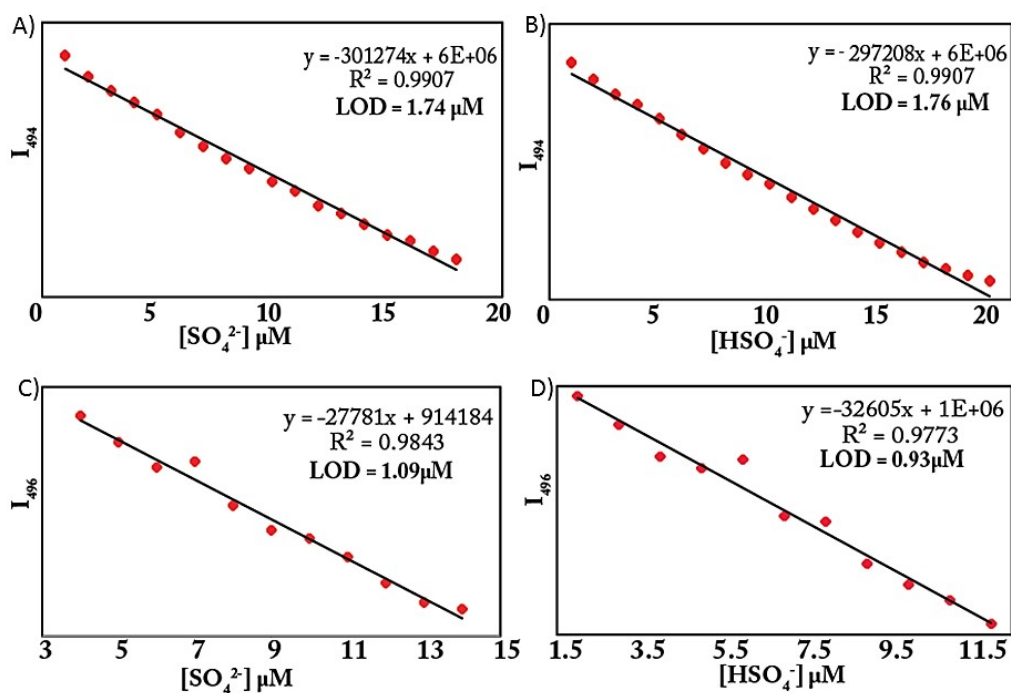


Figure S11. Fluorescence emission intensity of **A) R1** at 494 nm vs. SO_4^{2-} concentration **B) R1** at 494 nm vs. HSO_4^- concentration **C) R2** at 490 nm vs. SO_4^{2-} concentration **D) R2** at 490 nm vs. HSO_4^- concentration to calculate the limit of detection (LOD).

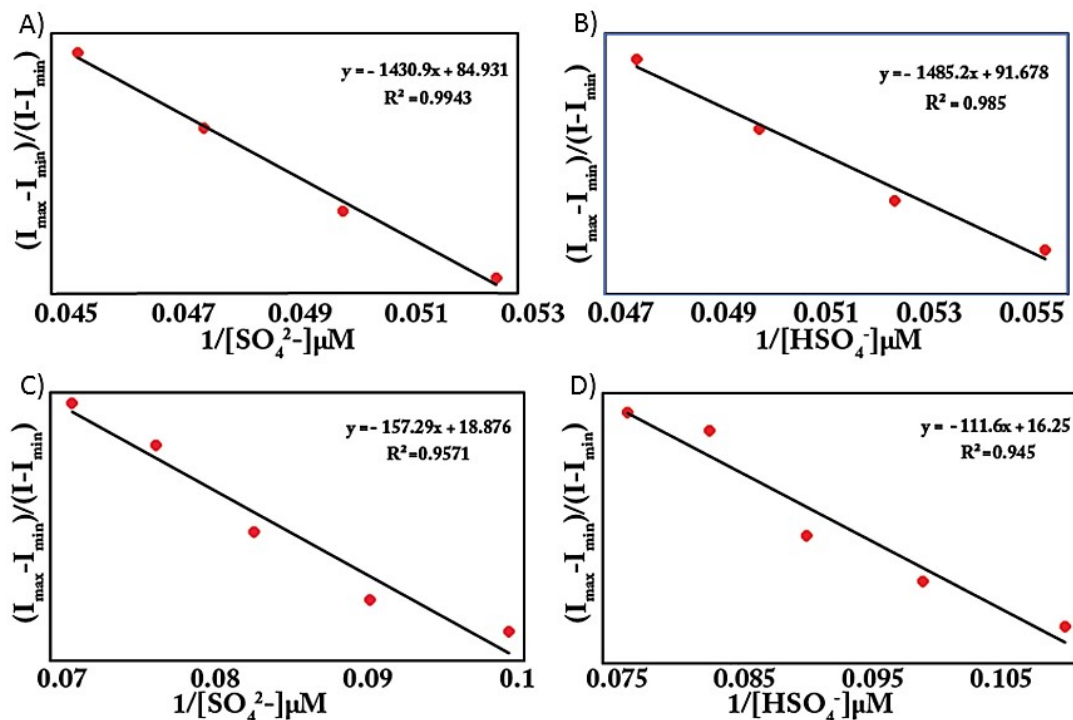


Figure S12. Benesi-Hildebrand plot for determination of binding constant of **A) R1** and SO_4^{2-} , **B) R1** and HSO_4^- , **C) R2** and SO_4^{2-} , **D) R2** and HSO_4^- .

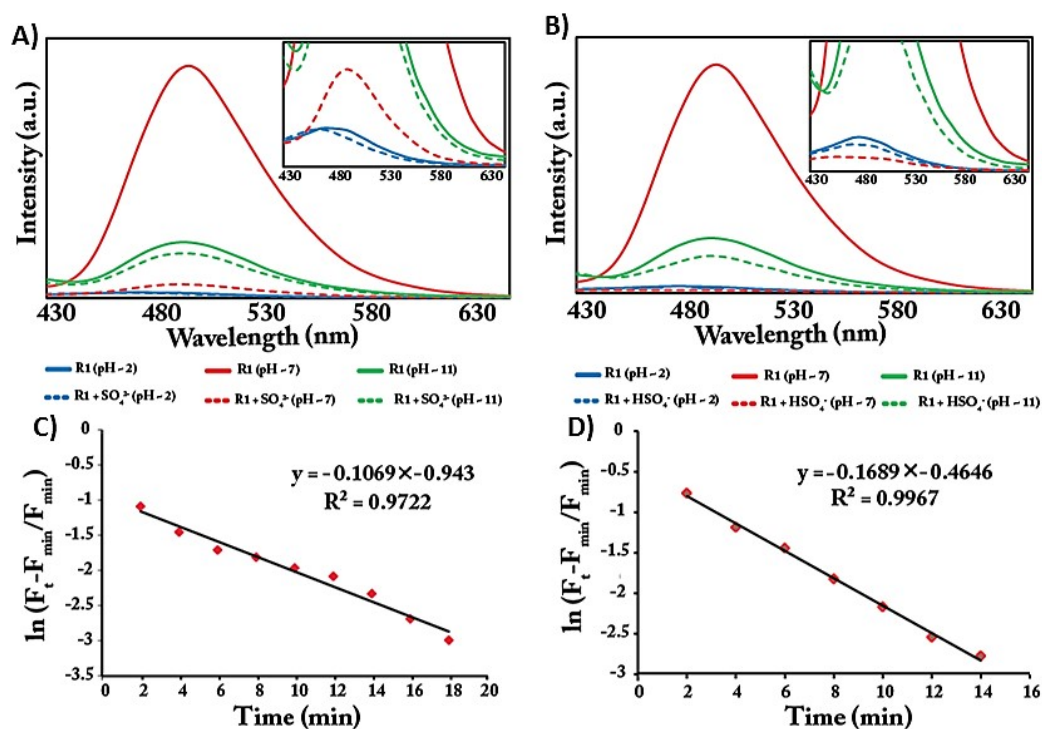


Figure S13: Fluorescence response of the probe **R1** (10 μM) in the absence or presence of **A) SO_4^{2-}** , **B) HSO_4^-** (100 μM) upon variation of pH in experimental solution and Fluorescence

intensity vs time (min), plotted using the first-order rate equation for **R1** recorded at 494 nm in presence of C) SO_4^{2-} , D) HSO_4^- (10 μM).

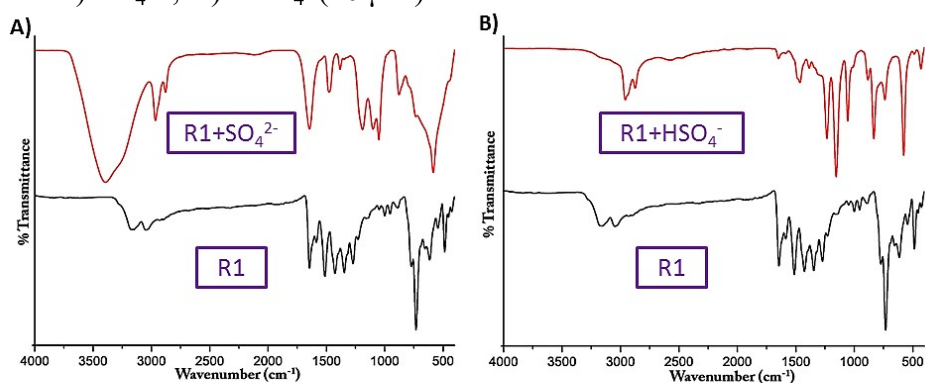


Figure S14. Comparison of FT-IR spectra of A) **R1** and **R1+ SO_4^{2-}** , B) **R1** and **R1+ HSO_4^-** .

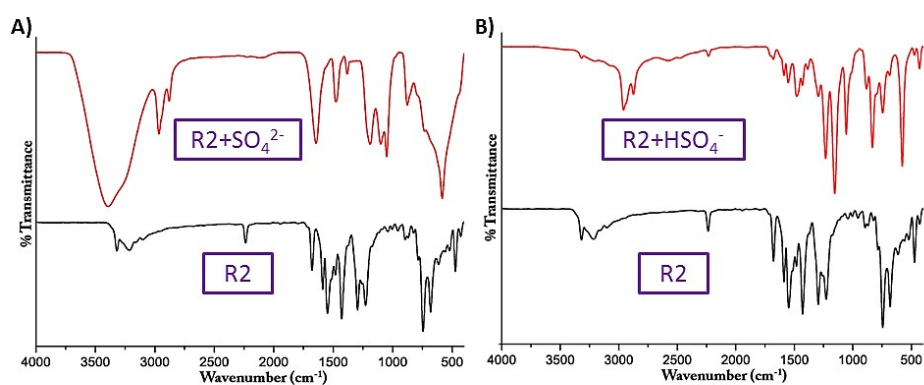


Figure S15. Comparison of FT-IR spectra of A) **R2** and **R2+ SO_4^{2-}** , B) **R2** and **R2+ HSO_4^-** .

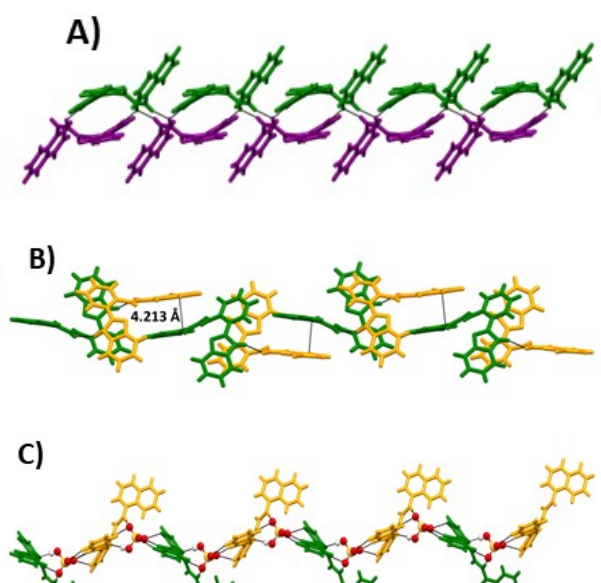


Figure S16. Self-assembled architecture of A) receptor **R1**, B) receptor **R2**, and c) complex **R1.HSO₄**.

Table S1: A representative comparison of the detection limits and binding constant values along with the receptor and solvent system used for the detection of $\text{SO}_4^{2-}/\text{HSO}_4^-$.

Sl. no.	References	Receptors	Solvent system	LOD (μM)	Binding Constant (M^{-1})
1.	Present work	neutral benzimidazole based urea receptors	100% water	1.74/1.76 and 1.09/0.93	$14.31 \times 10^8 / 14.85 \times 10^8$ and $1.57 \times 10^8 / 1.12 \times 10^8$
2.	Chemical Communications, 2009, 7128-7130	coumarin-based derivative	aqueous solution	3.75	4.86×10^4
3.	Organic letters, 2011, 13, 24, 6432–6435	bisferrocene-benzobisimidazole triad	Ethanol	6.58	3.95×10^5
4.	Analytical Methods, 2014,6, 9030-9036	Fluorescent organic nanoparticles of tripodal receptor	Aqueous medium	1.12	6.68×10^7
5.	RSC Advances, 2015, 5, 50532	copper(II) complex of quinazoline based ligand	water : DMSO (9 : 1, v/v)	3.18×10^{-1}	1.4×10^5
6.	Spectrochimica Acta Part A: Molecular and Biomolecular Spectroscopy, 2017, 180, 44–50	rhodamine 6G hydrazide receptor	Methanol	3.72	5353
7.	Journal of Photochemistry & Photobiology A: Chemistry 2019, 376, 146–154	oxindole-based probes	$\text{CH}_3\text{CN}/\text{H}_2\text{O}$ (7:3/v:v)	8.9	1.21×10^5
8.	Spectrochimica Acta Part A: Molecular and Biomolecular Spectroscopy, 2019, 213, 73–82	Azaindole-BODIPYs	acetonitrile	75.6 and 44.27	1.87×10^5 and 6.13×10^5
9.	Inorganica Chimica Acta, 2020, 511, 119794	dinuclear Zn (II) complex	3:2 v/v MeOH/water in HEPES buffer	Not reported	1.85×10^5
10.	New Journal of Chemistry, 2022,46, 18973-18983	diindolylarylmethane (DIAM)-based probes	Aqueous medium	6.2 ppb	Not reported

Explanation for the high R factor in receptor R2::

Response: The crystal of receptor **R2** diffracted extremely weakly which resulted in high R factor. Several attempts were made by using different crystallisation methods to grow better diffracting crystal of receptor **R2**, although it was unsuccessful.

Table S2: Crystallographic parameters and refinement data of the free receptors and the anionic complex.

Parameters	R1	R2	R1.HSO ₄
formula	C ₂₄ H ₁₈ N ₄ O	C ₂₁ H ₁₅ N ₅ O	C ₄₀ H ₅₅ N ₅ O ₅ S
fw	378.42	353.38	717.95
cryst syst	triclinic	orthorhombic	orthorhombic
space group	P -1	P 21 21 21	P c a 21
a (Å)	7.602(2)	16.878(9)	18.1980(14)
b (Å)	10.285(3)	24.478(13)	11.6386(9)
c (Å)	12.821(4)	8.566(5)	18.3823(14)
α (deg)	88.415(8)	90	90
β (deg)	87.473(8)	90	90
γ (deg)	73.566(8)	90	90
V (Å ³)	960.4(5)	3539(3)	3893.4(5)
Z	2	8	4
DC (g cm ⁻³)	1.309	1.326	1.225
μ (Mo Kα) (mm ⁻¹)	0.083	0.086	0.132
F (000)	396.0	1472.0	1544.0
T (K)	296 K	297 K	295 K
θ _{max} (deg)	24.995	24.995	24.999
total no. of rflns	16242	51084	99620
no. of indep rflns	3333	6226	6855
no. of obsd rflns	2818	4974	5128
no.of params refined	274	495	472
R1, I > 2σ(I)	0.0388(2818)	0.0809(4974)	0.0628(5128)
wR2, I > 2σ(I)	0.1470(3333)	0.2132(6226)	0.1875(6855)
GOF (F ²)	1.087	1.074	1.165
CCDC no.	2285005	2285016	2285018

Table S3: Hydrogen bonding distances (Å) and Bond angles (°) in the neutral receptors and the anionic complex.

Ligand/Complex	D H...A	d(D...H)/Å	d(H...A)/Å	d(D...A)/Å	<D-H...A/	Symmetry codes
R1	N1-H1N...O1	0.97 (2)	1.90 (2)	2.8632 (18)	174.7 (19)	-x, 1-y, 1-z
	N3-H3N...N2	0.883 (17)	2.113 (16)	2.7834 (19)	132.1 (14)	x, y, z
	N4-H4N...O1	0.902 (19)	1.969 (19)	2.8707 (17)	177.8 (15)	-x, 2-y, 1-z
	C12-H12...O1	0.93	2.58	2.897 (2)	100	x, y, z
	C21-H21...N4	0.93	2.56	2.873 (2)	100	x, y, z
R2	N1-H1N...O2	1.04 (12)	1.98 (12)	2.901 (9)	145 (9)	x, y, z
	N3-H3N...N2	0.86	2.22	2.787 (9)	124	x, y, z
	N4-H4N...N5	0.86	2.24	3.087 (9)	170	x, y, 1+z
	N6-H6N...O1	0.94 (5)	2.00 (5)	2.886 (9)	157 (4)	x, y, z
	N8-H8N...N7	0.86	2.21	2.734 (9)	119	x, y, z
	N9-H9N...N10	0.86	2.15	2.995 (9)	167	x, y, -1+z
	C12-H12...O1	0.93	2.49	2.896 (9)	107	x, y, z
	C16-H16...O1	0.93	2.20	2.802 (9)	122	x, y, z
	C30-H30...N6	0.93	2.60	2.909 (11)	100	x, y, z
	C33-H33...O2	0.93	2.53	2.898 (9)	104	x, y, z
	C41-H41...O2	0.93	2.35	2.870 (9)	115	x, y, z
	R1.HSO₄	N1-H1N...O3	0.76 (7)	2.04 (7)	2.796 (8)	172 (6)
O2-H2O...N2		0.78 (9)	1.88 (9)	2.661 (8)	177 (9)	1/2-x, y, -1/2+z
N3-H3N...N2		0.86	2.26	2.892 (7)	131	x, y, z
N3-H3N...O4		0.86	2.58	3.316 (7)	144	1/2-x, y, 1/2+z
N4-H4N...O4		0.86	2.05	2.901 (7)	170	1/2-x, y, 1/2+z
C1-H1...O5		0.93	2.51	3.342 (9)	149	x, y, z
C12-H12...O1		0.93	2.34	2.851 (9)	114	x, y, z
C16-H16...O1		0.93	2.53	2.915 (8)	105	x, y, z
C21-H21...N4		0.93	2.58	2.883 (9)	100	x, y, z
C23-H23...O1		0.93	2.56	3.448 (8)	159	-x, -y, 1/2+z
C34-H34B...O1		0.97	2.54	3.464 (11)	159	-x, -y, -1/2+z

References

- [1] Parker C A, Rees W T. Correction of fluorescence spectra and measurement of fluorescence quantum efficiency. *Analyst* 1960; 85 (1013): 587-600.
- [2] Rana A, Gogoi C, Ghosh S, Nandi S, Kumar S, Manna U, Biswas S. Rapid recognition of fatal cyanide in water in a wide pH range by a trifluoroacetamido based metal–organic framework. *New J Chem* 2021; 45 (43): 20193-20200.